Available online at www.sciencedirect.com

ScienceDirect

Energy Procedia 148 (2018) 194–201

Energy Procedia

www.elsevier.com/locate/procedia

73rd Conference of the Italian Thermal Machines Engineering Association (ATI 2018), 12–14 September 2018, Pisa, Italy

Investigation of a pressure compensated vane pump

F. Fornarelli[a], A. Lippolis[a] *, P. Oresta[a], A. Posa[b]

[a]*Dipartimento di Meccanica, Matematica e Management – Politecnico di Bari*
[b]*CNR-INM, Institute of Marine Engineering, Roma, Italy*

Abstract

Variable displacement hydraulic machines offer a very promising alternative and energy saving solution for many applications in mobile machines, robots and other applications. In the present paper a vane pump will be theoretically analyzed using the software AMESim and/or MATLAB/Simulink, in order to estimate the friction forces and volumetric efficiency loss without hardworking experimental tests. The friction forces taken into account by our model are the friction between vanes and rotor slots and that between vanes and eccentric pump stator. The same design parameters affect the volumetric and mechanical efficiency, whose behavior has been reported and discussed. The behavior of the machine is analyzed and discussed at different angular velocities and pressure regimes.

Keywords: Vane pump, Performance optimization.

1. INTRODUCTION

Vane pumps offer a very important energy saving solution in many scenarios, especially for lubrication of internal combustion engines [1, 3, 10, 12, 14, 15, 16], but also in mobile machines, robots and other fields. Over the years, several authors tried to propose accurate models: The first papers date back to 1986 by Karmel [6, 7, 8, 9]. Those

* Corresponding author. Antonio Lippolis Tel.: +39 0994733317; fax: +0-000-000-0000
E-mail address: lippolis@poliba.it

10.1016/j.egypro.2018.08.068

works were focused especially on the internal pressure distribution typical of this class of pumps and equivalent forces and torque. The pressure ripple was studied by Jang et Al. [5] e Mucchi et Al. [11], while the paper by Rundo et Al. [13] deals with the geometry assessment of variable displacement vane pumps. Vane pumps are also utilized in many fields outside of hydraulics, for example the paper by Bianchi et Al. [2] discusses about organic fluids for power conversion systems.

In the present paper a new model, developed using AMESim and/or Matlab software, is proposed. The same tools were utilized by the Authors to analyze an axial piston swashplate pump [4]. Our target in the present paper is to report a comprehensive computational tool, involving some simplifications, but accurate enough to help manufacturers in designing new vane pumps. Section 2 deals with the geometry of the pump analyzed here and section 3 presents its theoretical analysis. Sections 4 and 5 discuss the volumetric and torque losses, respectively. In section 6 the model, developed using AMESim software, is shortly presented together with the charts of pump performance as a function of the pump eccentricity.

Nomenclature

R_s	stator radius [mm]	F_{r1}, F_{r2}	Vane-Rotor normal forces [N]
R_r	rotor radius [mm]	C_{oil}	Vane torque due to oil [Nm]
e	eccentricity [mm]	L_c	Chamber energy required [J]
L_a	axial length [mm]		
s_v	vane thickness [mm]	**Greek**	
R_p	radius of the vane round end [mm]	θ	rotor angular position
V_v	Chamber volume	γ	angle between the vane middle line and the normal
p_a, p_m	Suction and delivery pressure [bar]		to the stator contact surface
F_N	Vane-Stator normal forces [N]	η_v	Volumetric efficiency
F_a	Vane-Stator friction forces [N]	η_m	Mechanical efficiency

2. PUMP GEOMETRY

The simulation model reported here is general. Nonetheless, in order to provide details about the geometry of the pump analyzed in the present paper, Fig. 1 shows pictures of some pump elements: the rotating body, an enlargement of a single vane, the stator and the pump assembly. In a sliding vane machine, a rotating cylinder (rotor) has a given number of axial grooves (slots) that host the parallelepiped vanes. The rotation of the rotor leads the vanes to slide along the slots and reach the inner surface of a bigger cylinder, the stator. This way, cells build up and their rotation allows the working fluid to move from suction to discharge. Front and back plate not only delimit the cells in the axial direction but also host the shaft bearings or bushes. The reference vane pump that will be presented in this paper is seven-vanes and its main geometrical parameters are reported in Table 1.

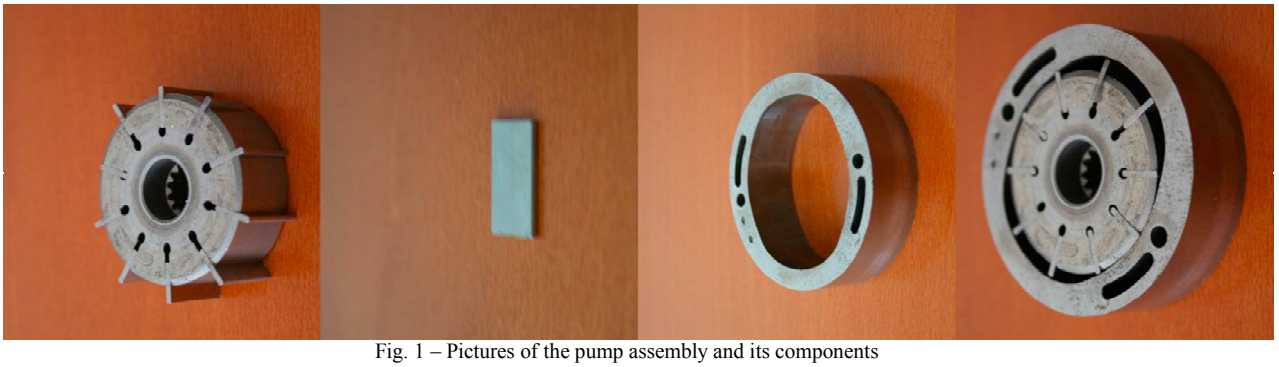

Fig. 1 – Pictures of the pump assembly and its components

Suction and discharge ports can be axially or radially located. For instance, in variable displacement devices ports are axial since the capacity is regulated acting on the eccentricity. This parameter, defined as length of the segment that connects stator and rotor centers, together with angular ports positioning, is fundamental for a correct sliding vane machine design. Indeed, the eccentricity affects the angular volume evolution with potential detrimental effects on machine performance. In particular, a small eccentricity leads to lower volumetric efficiency, while values of eccentricity close to the maximum one produce large angular volume variations. However, due to the incompressible nature of the working fluid, even slight volume variations, when the chamber volume is not in contact with the suction/discharge environments, are discouraged for pumps, since they would lead to pressure and torque peaks that eventually would shorten the lifetime of the device. In pumps, suction and discharge ports are usually spaced of an angle equal to the angular width of the cell, which essentially depends on the number of vanes. The theoretical values should be corrected taking into account the thickness of the vane.

Table 1 - Design parameters.

Rotor diameter 40 [mm]	Vane thickness 1 [mm]
Stator diameter 47 [mm]	Number of vanes 7
Axial length 9 [mm]	Maximus displacement 2 [cm^3]

3. THEORETICAL ANALYSIS

Figure 2 shows an enlargement of the contact point between vane and stator, which is theoretically that between the rounded vane circumference and the stator circumference. This contact point in 3-D corresponds to a line. In the same figure the angle θ, equivalent to the rotor angular position, is reported. The normal to the vane and stator contact surfaces, straight line passing through the stator axis O_s and the rounded vane end axis O_c, forms a δ angle with the horizontal, which can be computed as below:

$$\overline{O_s O_c} = R_s - R_p \quad (1)$$

$$\overline{O_r O_c} = e\cos\vartheta + \sqrt{(R_s - R_p)^2 - e^2\sin^2\vartheta} \quad (2)$$

$$\gamma = \delta - \theta = \arcsin\left(\frac{e}{R_s - R_p}\sin\theta\right) \quad (3)$$

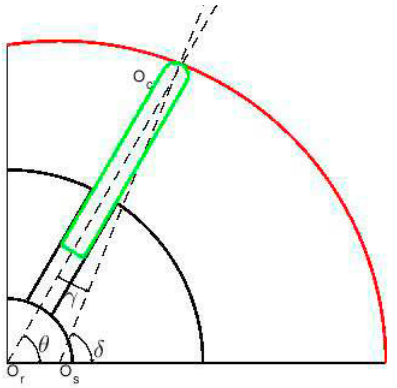

Fig. 2 – Vane-Stator interaction.

The angle γ, i.e. the angle between the vane middle line and the normal to the stator contact surface, depends on the angle θ, which is equal to zero when the chamber is at the horizontal position, while it is at its maximum when the vane is perpendicular to the straight line between the stator and rotor centers. Furthermore, γ depends on the rotor eccentricity and on the vane end radius. Fig. 3 shows the evolution of γ as a function of θ for various percentages of eccentricity from 0 to 10%. The vane end radius was assumed equal to half of vane thickness. The angle γ is rather small and in no case is larger than 6°.

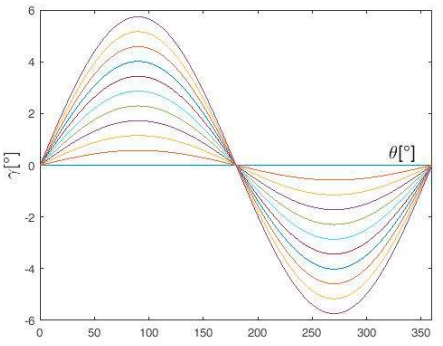

Fig. 3 –γ angle.

Fig. 4 deals with a case featuring an eccentricity of 10%. The red line shows the maximum value of γ, while the green line stands for the semi-angle of the vane end rounding, both as a function of the ratio between the vane end radius and the stator radius. Above a value of about 0.3 on the horizontal axis there is a rotation zone where the contact between the vane and the stator occurs at a corner of the vane which experiences a greater stress.

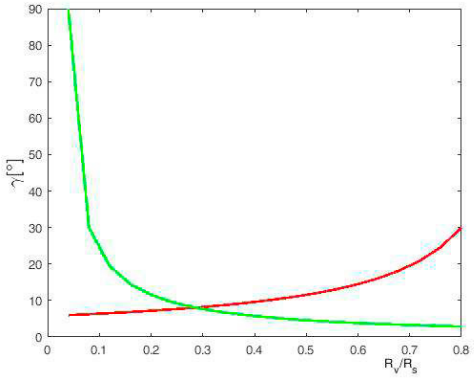

Fig. 4 – Vane end rounding effect.

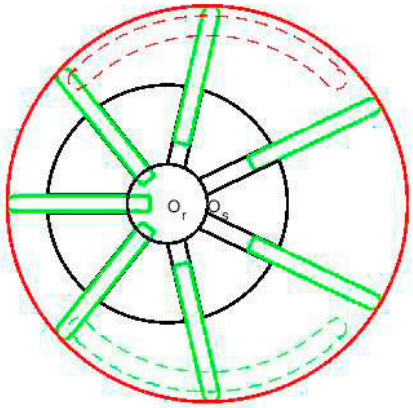

Fig. 5 – Pump cross section.

Fig. 5 shows a complete section of the pump with an indication of the suction and delivery connections, axially placed, represented via a dotted line. Assuming an anticlockwise rotation, the chamber on the right, symmetrically arranged relative to the horizontal diameter, features the maximum volume and just left the suction connection, in green, and is about to come in contact with the delivery environment, whose connection is in red. The distance between suction and delivery connections is important in order to reduce pressure and torque peaks. In Fig. 5, since the number of vanes is odd, i.e. 7, there is no chamber at the minimum volume, but two chambers on the left are near the minimum: the upper one has just left the delivery environment and is moving towards the minimum volume, while the lower one is already growing and going towards the suction connection.

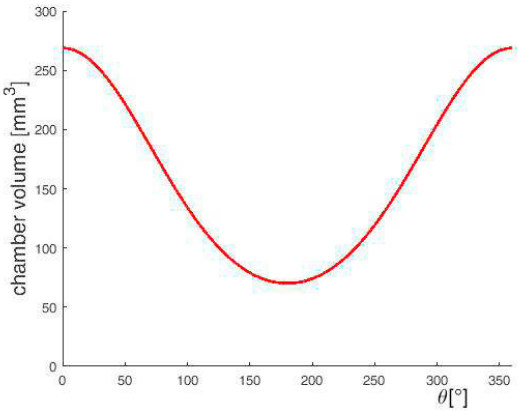

Fig. 6 – Chamber volume evolution.

Fig. 6 shows the evolution of the chamber volume as a function of the rotor angle θ. The angle θ is assumed equal to zero when the chamber is placed symmetrically on the right, see Fig. 5, corresponding to maximum chamber volume, while θ = 180° corresponds to the minimum volume. The suction and delivery connections must be circumferentially limited so that the chamber in the vicinity of both the maximum and minimum volume does not allow the passage of fluid from high pressure to the low pressure environments.

4. OIL COMPRESSIBILITY AND LEAKAGE LOSSES

In this section oil compressibility and leakages are discussed, being the main parameters influencing the volumetric efficiency of the pump. At the beginning of the delivery stroke, the volume of the chamber decreases, causing the increase of the oil pressure. This phenomenon is positive because the outlet pressure is high, compared to the suction pressure, and the pressure jump cannot be too abrupt. A gradual passage from the suction to the outlet pressure and vice versa requires an optimal design. Oil compressibility is just one of the reasons of the flow rate reduction, which is mainly due to the leakage inside the internal gaps. We can distinguish two main leakages phenomena: vane/rotor and vane/stator. The leakage due to vane/rotor clearance is caused by two main sources: one of them is the vane displacement pushing the oil into the gap between vane and rotor groove, the second source of leakage is the pressure gradient through the gap between the chamber pressure and the pump internal pressure. This latter effect is negligible during the suction phase, but it is more significant across the delivery phase.

Fig. 7 shows the main sources influencing the volumetric efficiency: the blue line takes into account only the volume variation inside the chamber when it passes from suction to discharge connections and vice versa. In fact, after the chamber has abandoned the contact with the suction environment, its volume continues to grow and a limited depression is created. Then, after the point of symmetry, the volume starts to decrease again and the pressure begins to rise. The opposite phenomenon occurs when the chamber leaves the delivery environment room and its volume keeps decreasing: there is a pressure peak, which in the figure is equal to about 40 [bar].

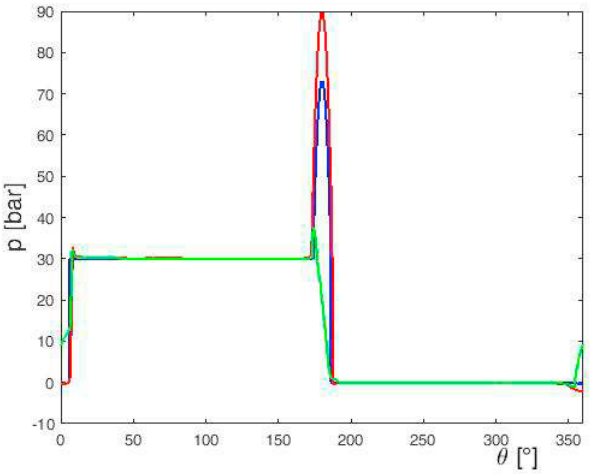

Fig. 7 – Pressure fluctuation.

The red line takes into account the pressure losses in the suction and discharge ports: when the chamber comes into contact with the delivery room, the passage window is very small and grows until the maximum value is reached, as shown in Fig. 8, where the delivery port area is in red and the suction area is in blue. In the first phase, there is an outflow from delivery environment to the pump chamber. The same process occurs from the red one, with a very small flow between pump chamber and suction environment: Differences between the blue and red lines in Fig. 7 are negligible. A third phenomenon is due to the leakage between a two contiguous chambers: leakage occurring between the vane tip and the pump stator. These leakages occur when a chamber is in contact with the suction environment, while the next one is in contact with the delivery environment and vice versa, in general when pressure differences exist between two adjacent pump chambers: all these phenomena are represented by the green line. In Fig. 7 during the passage from suction to delivery phases there is a gradual pressure increase, due essentially to the leakage from the previous chamber, already in contact with the delivery environment. In the passage from the delivery to the suction phases, a limited pressure peak is shown, since during the initial phase leakages are lower than the volume reduction. As a consequence, a pressure drop adjusting the chamber pressure to the suction pressure occurs, whose effect is obviously visible, since in this case the pressure peaks of the blue and red curves are not entirely distinguishable.

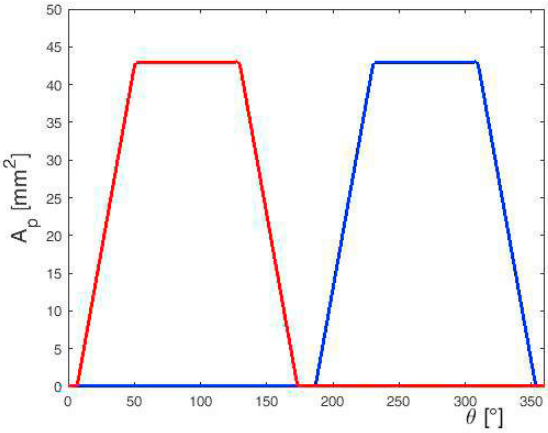

Fig. 8 – Suction and delivery ports areas.

Leakages are the main source of losses in terms of volumetric efficiency of vane pumps. In contrast, oil compressibility is much less important. In the example shown in Fig. 7 the volumetric efficiency is 94.44%, whereas the effect of oil compressibility is about 1%. It is well known that the volumetric efficiency depends on the delivery pressure and angular speed: the leakage rate is indeed proportional to delivery pressure and approximately independent of the angular speed, whereas the ideal flow rate is proportional to the angular speed. In Fig. 9 the volumetric efficiency was reported as a function of RPM for three different values of delivery pressure, 20 (blue line), 30 (red line) and 40 (green line) [bar], respectively.

5. MECHANICAL PERFORMANCE

The mechanical performance ideally depends on the pump displacement and the pressure drop between suction and delivery environments. The cycle work by the pump is higher than the ideal cycle, mainly because of the following phenomena:

1) The pressure inside the pump chambers is different from those in the suction and discharge environments;

2) The friction forces between vanes and pump stator;
3) The friction forces between the vane and the rotor clearance.

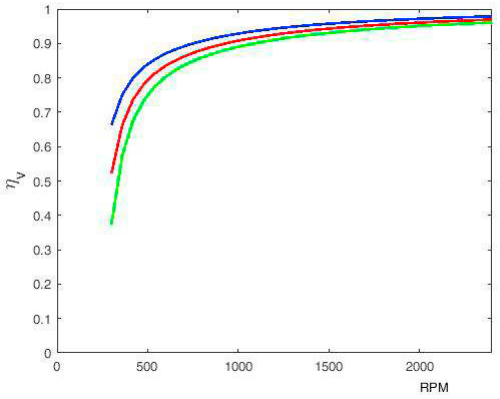

Fig. 9 – Volumetric efficiency

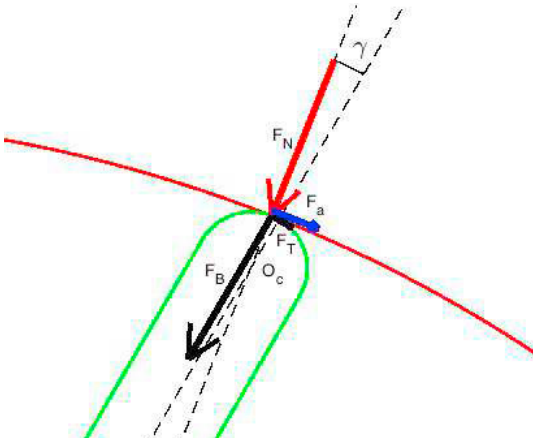

Fig. 10 – Friction forces between vane and pump stator

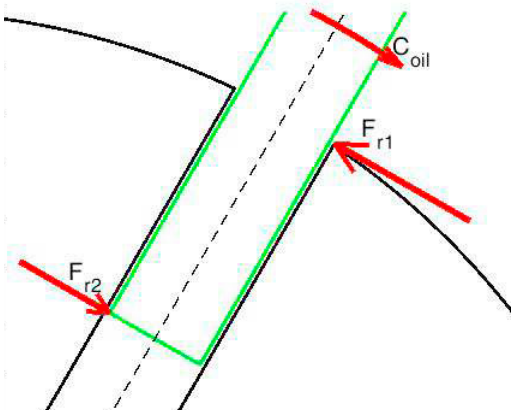

Fig. 11 – Friction forces between the vane and the rotor clearance

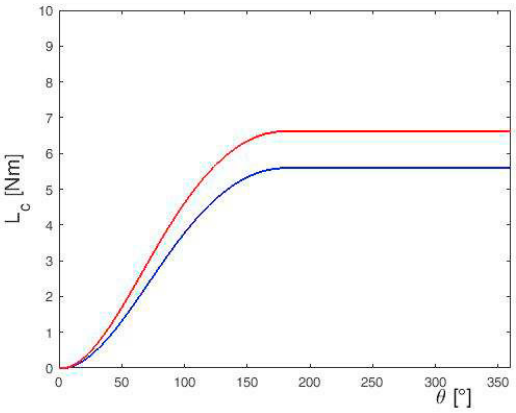

Fig. 12 – Work cycle of a pump vane.

Fig. 10 shows a close up view of the contact area between the vane and the stator, already shown in Fig. 2: the normal force F_N of the stator over the vane can be decomposed into a component F_B along the axis of the vane, which balances the centrifugal force and the inertial force, due to the radial acceleration, and a normal component F_T braking the rotor and balanced by the driving torque. To F_N, due to the friction, a tangential force F_a must be added, which can also be decomposed along the directions discussed above. The F_a component is much less significant because oil reduces substantially the friction forces.

Fig. 11 shows a close up view of the contact area between the rotor groove and the vane, which moves inside the same groove: the force of the oil pressure over the vane, especially when the pressure in the two adjacent chambers is different, tends to rotate the vane. This rotation determines two tangential forces, F_{r1} and F_{r2}, from the groove toward the vane, generating a torque that balances that due to the oil. The tangential forces F_{r1} and F_{r2} cause also the friction forces F_{a1} and F_{a2}. They are opposite to the vane motion along the radial direction and obviously dissipate energy.

Fig. 12 shows the work cycle that the drive shaft must provide to the pump chamber when the rotation angle changes. It is clear that the work mainly increases when the pump chamber is in contact with the delivery environment: the reduction of the chamber volume inevitably requires a flow rate and work supply. The work grows slightly in the first phase when the volume decreases even though the delivery lights have not yet been opened and in the last phase when the delivery lights have already been closed, but the chamber volume keeps decreasing. Over the last 180° of rotation the work keeps almost constant, but even in this phase there is a limited work growth, while

ideally work should be equal to zero. In Fig. 12 the blue line takes into account only the pressure inside the chamber, while the red line also takes into account the losses due to friction between vane and pump stator and rotor clearance.

Friction is the main source of losses in terms of mechanical efficiency of vane pumps. In contrast, pressure fluctuation is much less important. In the example shown in Fig. 13 mechanical efficiency is 90%, whereas the effect of pressure fluctuation is about 0.5%. In Fig. 13 mechanical efficiency was reported as a function of delivery pressure for three different values of RPM, 1200 (blue line), 2100 (red line) and 3000 (green line) [RPM], respectively. It is well evident from Fig. 13 that mechanical efficiency depends mainly on the angular speed, while the influence by the delivery pressure is much weaker.

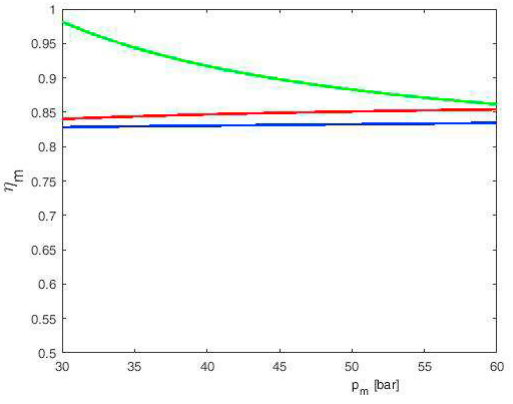

Fig. 13 – Mechanical efficiency.

6. PUMP SIMULATION MODEL

Each chamber presents the same behavior, therefore the AMESim model was developed only for one chamber in a supercomponent. Thus, the entire pump consists of the assembly of a number of supercomponents equal to the number of chambers/vanes. In Fig. 14 the scheme of a single supercomponent, including both volumetric leakages and mechanical losses, is presented. All forces applied to the pump vane component converge to the green element shown below. It is worth stressing the presence of pressure transducers, measuring both the pressure inside the chamber and the pressure in the suction and delivery environments.

The icon 1 stands for the number of chambers N, the icons 2 and 4 give the output of the system, which are torque and flow-rate, respectively. The icon 5 stands for the angular velocity of the pump in [RPM]. The icon 6 represents the number of the analyzed chamber, in the range 0÷N-1. The icon 3 stands for the simulation time.

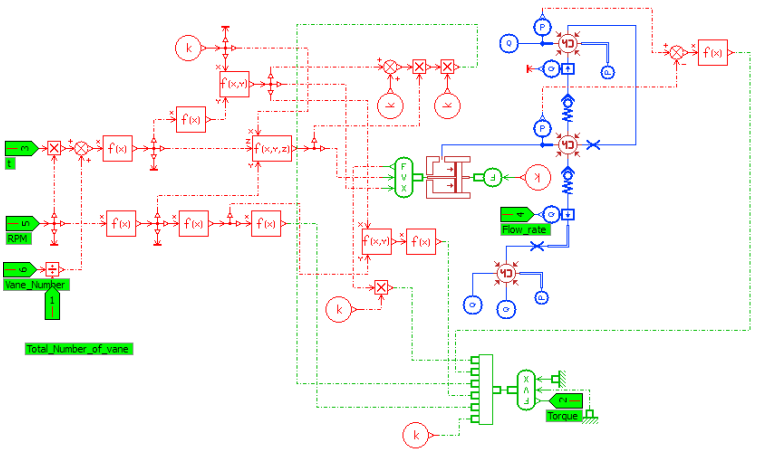

Fig. 14 – Ideal simulation model of a chamber in AMESim.

In fig. 15 a scheme of a seven vanes pump is reported, where each black icon represents one of the chambers. The parameter in the top left area in Fig. 14 represents the angular velocity that is, indeed, constant for each vane. The parameter on the left bottom area represents the number of vanes, that is equal to seven in this case. The only parameter linked to each supercomponent is the number of the corresponding chamber. In particular, in this case it goes from 0 to 6. The first chamber (0) has 0° phase shift, therefore the other chambers have a consecutive phase shift of (360°/7). The flow rates of each single supercompont converge on the left, where they are added to obtain the total pump flow rate sent to the delivery environment. The mechanical torques of each single supercompont converge on the right, where they are added in order to obtain the total torque.

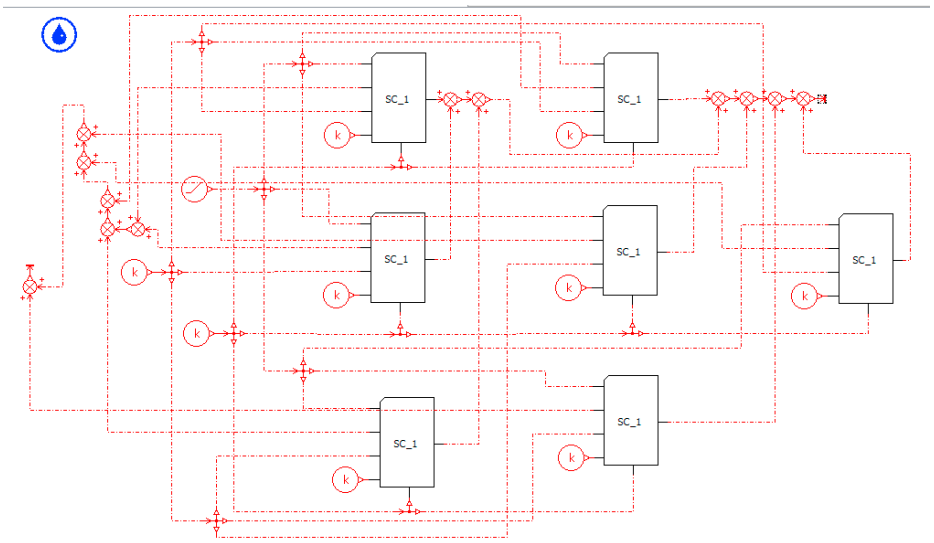

Fig. 15 Model of a 7-vanes pump.

References

[1] Barbarelli, S., Bova, S., & Piccione, R. (2009). Zero-Dimensional Model and Pressure Data Analysis of A Variable-Displacement Lubricating Vane Pump, Retrieved from www.scopus.com

[2] Bianchi, G., Fatigati, F., Murgia, S., & Cipollone, R. (2017). Design and analysis of a sliding vane pump for waste heat to power conversion systems using organic fluids. Applied Thermal Engineering, 124, 1038-1048. doi:10.1016/j.applthermaleng.2017.06.083

[3] Cantore, G., Paltrinieri, F., Tosetti, F., & Milani, M. (2010). Lumped Parameters Numerical Simulation of A Variable Displacement Vane Pump for High Speed ICE Lubrication, Retrieved from www.scopus.com

[4] Fornarelli, F., Lippolis, A., Oresta, P. & Posa, A. (2017). A computational model of axial piston swashplate pumps, Energy Procedia, Vol. 126, pp. 1147-1154, doi 10.1016/j.egypro.2017.08.314.

[5] Jang, J., Kim, K., Cho, M. & Han, D. (2002). The characteristics of pressure ripple in variable displacement vane pumps: Comparison between theory and experiment. Proceedings of the Institution of Mechanical Engineers, Part A: Journal of Power and Energy, 216(1), 89-96. doi:10.1243/095765002760024971

[6] Karmel, A. M. (1986). A study of the internal forces in a variable-displacement vane-pump-part I: A theoretical analysis. Journal of Fluids Engineering, Transactions of the ASME, 108(2), 227-232. doi:10.1115/1.3242567

[7] Karmel, A. M. (1986). A study of the internal forces in a variable-displacement vane-pump-part II: A parametric study. Journal of Fluids Engineering, Transactions of the ASME, 108(2), 233-237. doi:10.1115/1.3242568

[8] Karmel, A. M. (1988). Modeling and analysis of the dynamics of a variable-displacement vane-pump with a pivoting cam. Journal of Dynamic Systems, Measurement and Control, Transactions of the ASME, 110(2), 197-202. doi:10.1115/1.3152671

[9] Karmel, A. M. (1988). Stability and regulation of a variable-displacement vane-pump. Journal of Dynamic Systems, Measurement and Control, Transactions of the ASME, 110(2), 203-209. doi:10.1115/1.3152672

[10] Mancò, S., Nervegna, N., Rundo, M., & Armenio, G. (2004). Modelling and simulation of variable displacement vane pumps for IC engine lubrication. SAE Technical Papers, doi:10.4271/2004-01-1601

[11] Mucchi, E., Cremonini, G., Delvecchio, S., & Dalpiaz, G. (2013). On the pressure ripple measurement in variable displacement vane pumps. Journal of Fluids Engineering, Transactions of the ASME, 135(9) doi:10.1115/1.4024110

[12] Rundo, M. (2010). Piloted displacement controls for ICE lubricating vane pumps. SAE International Journal of Fuels and Lubricants, 2(2), 176-184. doi:10.4271/2009-01-2758

[13] Rundo, M. and Nervegna, N., 2007. Geometry assessment of variable displacement vane pumps. Journal of Dynamic Systems, Measurement and Control, 129 (4), 446–455.

[14] Rundo, M., & Nervegna, N. (2015). Lubrication pumps for internal combustion engines: A review. International Journal of Fluid Power, 16(2), 59-74. doi:10.1080/14399776.2015.1050935

[15] Truong, D. Q., Ahn, K. K., Trung, N. T., & Lee, J. S. (2013). Performance analysis of a variable-displacement vane-type oil pump for engine lubrication using a complete mathematical model. Proceedings of the Institution of Mechanical Engineers, Part D: Journal of Automobile Engineering, 227(10), 1414-1430. doi:10.1177/0954407013491896

[16] Truong, D. Q., Ahn, K. K., Trung, N. T., & Lee, J. S. (2013). Theoretical investigation of a variable displacement vane-type oil pump. Proceedings of the Institution of Mechanical Engineers, Part C: Journal of Mechanical Engineering Science, 227(3), 592-608. doi:10.1177/0954406212464615